ACS OMEGA

Open Access

http://pubs.acs.org/journal/acsodf

Article

Enhancement of Vitamin C's Protective Effect against Thimerosal-Induced Neurotoxicity in the Cerebral Cortex of Wistar Albino Rats: An *In Vivo* and Computational Study

Published as part of ACS Omega virtual special issue "3D Structures in Medicinal Chemistry and Chemical Biology."

Amr Hassan,* Reham Mohsen, Ahmed Rezk, Gabrielle Bangay, Patrícia Rijo, Mona F. M. Soliman, Mohamed G. A. Hablas, Khalifa AbdulRazik K. Swidan, Tahseen S. Mohammed, Mohammad A. Zoair, Abir A. Khalil Mohamed, Tamer I. Abdalrhman, Ahmad M. Abdel-aleem Desoky, Dalia D. Mohamed, Doaa D. Mohamed, Ahmed I. Abd El Maksoud, and Aly F. Mohamed

Cite This: https://doi.org/10.1021/acsomega.3c07239

Read Online

ACCESS | Metrics & More | Article Recommendations

ABSTRACT: Vitamin C was examined to ameliorate the neurotoxicity of thimerosal (THIM) in an animal model (Wistar albino rats). In our work, oxidative and antioxidative biomarkers such as SOD, LPO, and GSH were investigated at various doses of THIM with or without concurrent vitamin C administration. Furthermore, the adverse effects of THIM on hepatic tissue and cerebral cortex morphology were examined in the absence or presence of associated vitamin C administration. Also, we studied the effect of vitamin C on the metallothionein isoforms (MT-1, MT-2, and MT-3) *in silico* and *in vivo* using the RT-PCR assay. The results showed that the antioxidant biomarker was reduced as the THIM dose was raised and vice versa. THIM-associated vitamin C reduced the adverse effects of the THIM dose. The computation studies demonstrated that vitamin C has a lower ΔG of −4.9 kcal/mol compared to −4.1 kcal/mol for THIM to bind to the MT-2 protein, which demonstrated that vitamin C has a greater ability to bind with MT-2 than THIM. This is due to multiple hydrogen bonds that exist between vitamin C and MT-2 residues Lys31, Gln23, Cys24, and Cys29, and the sodium ion represents key stabilizing interactions. Hydrogen bonds involve electrostatic interactions between hydrogen atom donors (*e.g.*, hydroxyl groups) and acceptors (*e.g.*, carbonyl oxygens). The distances between heavy atoms are typically 2.5−3.5 Å. H-bonds provide directed, high-affinity interactions to anchor the ligand to the binding site. The five H-bonds formed by vitamin C allow it to form a stable complex with MT, while THIM can form two H-bonds with Gln23 and Cys24. This provides less stabilization in the binding pocket, contributing to the lower affinity compared to vitamin C. The histopathological morphologies in hepatic tissue displayed an expansion in the portal tract and the hepatocytes surrounding the portal tract, including apoptosis, binucleation, and karyomegaly. The histopathological morphologies in the brain tissue revealed a significant decrease in the number of Purkinje cells due to THIM toxicity. Interestingly, THIM toxicity was associated with hemorrhage and astrogliosis. Both intracellular and vasogenic edema appeared as the concentrations of THIM rose. Finally, vitamin C ameliorated the adverse effect on the cerebral cortex in Wistar albino rats.

INTRODUCTION

Thimerosal (THIM) is defined as an organomercurial compound, sodium ethylmercury (Hg) thiosalicylate ($C_9H_9HgNaO_2S$). Mercury contributes 50% of its weight. THIM dissolves in saline solution and is fragmented into ethyl-Hg hydroxide and ethyl-Hg chloride.[1] THIM has entered the vaccine industry as a preservative, especially in pediatric vaccines, without being screened and monitored for its safety in developing organisms.[2] THIM exists in different vaccines, such as influenza vaccine Fluvirin MDV produced by Novartis.[3,4] Also, a HepA/HepB vaccine called Twinrix, produced by GlaxoSmithKline, the pharmacodynamics and pharmacokinetic properties of ethylmercury showed increased lipophilicity with low water solubility, which increased its toxicity profile.[5] Initially, it is dissociated in the bloodstream

Received: September 20, 2023
Revised: December 29, 2023
Accepted: January 9, 2024

into ethylmercury; after that, the ethylmercury transforms into other forms. Furthermore, mercury has an adverse effect on the brain's ability to cross the blood−brain barrier (BBB). In mercury intoxication, multiple systems are targeted.[6,7] In mercury intoxication, multiple systems are targeted.[6] Also, mercury degenerates neuronal axons because it induces disruption of the structure of the axon or neurite, causing it to depolymerize. The function of guanosine triphosphate (GTP) is to provide energy, which keeps the tubulin proteins linked together by binding to the tubulin.[8] However, when Hg exists in the brain, it replaces GTP by binding to the GTP-binding site of the beta subunit of the linked tubulin proteins.[9] Interestingly, the presence of mercury at the GTP-binding sites stops the supporting energy transfer, which breaks the links between the tubulin subunits and disrupts this scaffolding.[10] The toxicity mechanism of mercury depends on the binding sulfhydryl group in the proteins and peptides distributed throughout the body.[11] Metallothionein (MT) is a low-molecular-weight protein enriched with cysteine, with fewer disulfide bonds. It includes four isoforms. MT-1 and MT-2 exist in glial and astrocyte cells and they function as the elimination of free radicals, acceleration of cell proliferation, storage of essential metals, and reduction of adverse effects of heavy metals. While MT-3 was detected recently in a neuron rat's brain,[12] recent articles documented that elevated MT-3 is related to IL-3, TGF-α, and EGF while it is up−down by IL-6, kainite, and dexamethasone.[12,13] The role of MT-1 and MT-2 is detoxification, while MT-3 protects and repairs neurons.[13] Traumatic brain injury (TBI) can activate brain edema throughout the BBB, which leads to vasogenic and cytotoxic edema, ultimately leading to neuronal death.[14,15] Vitamin C is an essential nutrient supplement that contributes to multiple biological functions. Also, it enters into different physiological functions, such as in the transformation of the neurotransmitter dopamine to norepinephrine. It contributes to reducing ferric Fe^{3+} to ferrous Fe^{2+} ions.[16] Vitamin C is a potent antioxidant that scavenges free radicals by rapid electron transfer and inhibits lipid peroxidation (LPO) in the brain.[17] The current study focuses on the effects of ascorbic acid (vitamin C) on the biochemical and histopathological effects of THIM in the hepatic and brain tissues of male Wistar albino rats after administration.

MATERIALS

Thiomersal, vitamin C, EDITA, hematoxylin and eosin (H&E) staining, staining powder, formaldehyde 37−40%, sodium chloride powder, and sulfuric acid were obtained from Sigma-Aldrich, United States, and phosphate-buffered saline from MERCK, Germany.

METHODS

Animals and Experimental Design. We followed the entire Council Directive of the European Communities (Directive 2010/63/EU of September 22, 2010). According to the Institutional Animal Care with oversight of the Faculty of Veterinary Medicine, University of Sadat City (ethical approval number: VUSC-043-1-22), the experimental procedure was performed according to the Animal Protocols Evaluation Committee's affirmative opinion. Thirty-five male Wistar albino strains rats were obtained from the animal house of VACSERA, Giza, Egypt, at the age of one and a half months and weighed 150−200 g. The rats were housed in standard conditions, with a room temperature range of 22−24 °C for a 12 h light/12 h dark cycle with food and water. Rats were given nutrient-dense diet of dry food diet, and water was freely available. The rats were separated into seven groups of five rats per group for the experiment.

Animal Experimentation. Thirty male Wistar albino rats were divided into six groups of five animals, each treated for 20 days. Group 1 rats were given distilled water, group 2 rats were given 25 μg/mL thiomersal, and group 3 animals were given 50 μg/mL thiomersal, respectively. Animals in group 4 were given 25 μg/mL body weight of thiomersal and 5 μg/mL body weight of vitamin C, while group 5 animals were administered with 50 μg/mL thiomersal and 5 μg/mL vitamin C, and group 6 rats were administered with 5 μg/mL vitamin C only. The administration was done by injection via IP, three times at 10-day intervals, and lasted 20 days.

Animals Sacrifice. At the end of the experiment, on the 21st day, the animals were fasting for 12 h, and an acceptable euthanasia method was applied to sacrifice the mice, according to Hassan *et al.* 2021.[18] The tissues were routinely processed and stained using hematoxylin and eosin, while the cerebellum was removed and fixed in Bouin's fluid.

***In Vivo* Study.** *Collection of Heart, Liver, and Serum.* After the rats were anesthetized and sacrificed, all of the body organs, such as the liver, kidney, and heart, were collected and weighed. The hepatic tissues were collected and frozen at −80 °C for further analysis. Also, the blood samples were collected by intracardiac puncture and centrifugalized to separate the serum, then tucked in heparinized tubes. The serum was mixed gently by inverting 2−3 times and incubating at 4 °C for 2−3 h.

Preparation of Tissue Homogenate. The tissue homogenate of the rat's organs, such as the liver and heart, was prepared by putting the wet tissue (1 g) in 10-fold (w/v) 0.05 M ice-cold phosphate buffer (pH 7.4) and homogenizing it with a Teflon homogenizer. Then, 0.2 mL of homogenate was used to test the TBARS. The main part of the homogenate was separated into two parts. One part was mixed with 10% TCA in a ratio of 1:1. Then it was centrifuged at 5000 rpm at 4 °C for 10 min. After the centrifugation, the supernatant was separated and used to investigate the GSH. The other part of the homogenate was centrifuged at 15,000 rpm at 4 °C for 60 min; after the centrifugation, the supernatant was separated and used to evaluate the SOD.

Biochemical Analysis. *Blood Lipid Profile Analysis.* The lipid profile was measured by applying kits from Accurex Biomedical Pvt. Ltd. Low-density lipoprotein cholesterol (LDL-C) and very LDL-C (VLDL-C) are calculated by Friedwald's formula.[19]

Evaluation of Tissue Markers of Oxidative Stress

Lipid Peroxidation Assay. Preparation of the rat liver homogenate was done as follows. After anesthetizing the adult Wistar albino rats (170−200 g) with sodium pentobarbitone (35 mg kg^{-1}), they underwent excision of one lobe of the liver and washing with a 0.9% NaCl solution. The tissue homogenate was prepared by adding 1 g of wet tissue to 10-fold of (w/v) 0.05 M ice-cold phosphate buffer (pH 7.5) and then homogenizing the mixture by using a Teflon homogenizer. The homogenate tissue was used to investigate thiobarbituric acid reactive substances (TBARSs).

TBARS Assay. The LPO of liver homogenate was evaluated by applying the Kumari method.[20] In brief, the liver homogenate tissue (0.25 mL) was mixed with 0.1 mL of

https://doi.org/10.1021/acsomega.3c07239
ACS Omega XXXX, XXX, XXX−XXX

Table 1. List of the Primers Use by RT-PCR

primer name	forward primer	reverse primer
MT-1	5′- CTCCGTAGCTCCAGCTTCAC-3	5′-AGGAGCAGCAGCTCTTCTTG-3′
MT-2	5′-ACTTGTCGGCCGCCTCTTTG-3′	5′-CGACTATCCCTTCAAACCGA-3′
MT-3	5′-GCTGCAAATGCACGAACTG-3′	5′-CCCTCTTCACCTTTGCACAC-3′
GAPDH	5′-AACGACCCCTTCATTGAC-3′	5′-TCCACGACATACTCAGCAC-3′

Table 2. Body Weight Gain of Control Male Rats Treated with a Different Concentration of Thiomersal and Vitamin C[a]

parameter	experimental group				
	NC	group 1	group 2	group 3	group 4
initial body weight (g)	34.2 ± 2.2	33.5 ± 1.9	33.1 ± 2.1	32.3 ± 1.1	32.8 ± 1.1
final body weight (g)	33.4 ± 1.6	21.1 ± 1.1[b]	19.1 ± 0.9[b]	26.7 ± 1.3[b]	30.1 ± 1.0

[a]NC, normal control; group 1: thiomersal (25 μg/mL); group 2: thiomersal (50 μg/mL); group 3: thiomersal (50 μg/mL) with vitamin C (5 μg/mL); group 4: vitamin C (5 μg/mL). [b]Statistically significant differences from control: *$p < 0.05$.

Tris HCL buffer (pH 7.2), 0.05 mL of 0.1 mM ascorbic acid, 0.05 mL of 4 mM FeCl2 solution, and 0.05 mL of the test extracts. All extracts were tested at five different concentrations (5−80 μg/mL). The mixture was incubated at 37 °C for 1 h, and then 1.5 mL of 0.8% (w/v) 2-thiobarbituric acid, 1.5 mL of 20% acetic acid, and 0.2 mL of 8.1% (w/v) sodium dodecyl sulfate were added to the reaction mixture. The mixture was filled up to 4.0 mL with distilled water and heated at 95 °C for 60 min. After cooling with tap water, 1.0 mL of distilled water and 5.0 mL of a mixture of n-butanol and pyridine (15:1, v/v) were added. The mixture was shaken vigorously. The absorbance was measured at 532 nm in a spectrophotometer (Beckman, United Kingdom). Ascorbic acid and trolox were utilized as standards.[20]

Determination of Reduced Glutathione Level. Reduced glutathione level (GSH)was investigated by the Ellman method (1959).[21]

Evaluation of Superoxide Dismutase. Superoxide dismutase (SOD) was investigated by the Marklund method.[22]

Estimation of Nitric Oxide. Nitric oxide (NO) radical scavenging assay was carried out as per the method of Green *et al.*[23]

Study of the Effect of Vitamin C Associated with Thimerosal on MT in Cerebellum and Cerebrum Using Reverse Transcriptase-Polymerase Chain Reaction. The study was done according to Minami *et al.*[12] with some modifications in the methodology and concentrations. To observe the dose-dependent effects of THIM on the mouse cerebrum and cerebellum, 25 μg/mL thiomersal, 50 μg/mL thiomersal, 25 μg/mL thiomersal, and 5 μg/mL vitamin C, or 50 μg/mL thiomersal, 5 μg/mL vitamin C, and 5 μg/mL vitamin C were subcutaneously injected and animals were anesthetized by pentobarbital after 6 h, after which the cerebrum and cerebellum were removed. In the control group, mice were injected with 10 mL/kg saline, and the organs were removed 6 h after the injection[12]

Quantitative Reverse Transcriptase-Polymerase Chain Reaction. Total RNA was extracted from the cerebrum and cerebellum solution using a Fast RNA Pro Green Kit according to the manufacturer's protocol. A two-step multiplex quantitative reverse transcriptase-polymerase chain reaction (RT-PCR) method was used to determine the gene expression. The pairs of primers for mouse MT-1, MT-2, MT-3, and GAPDH were designed using Primer (Applied Biosystems), as summarized in Table 1. Reactions were performed in a 25 μL volume with forward primer, reverse primer, SYBR Green Realtime PCR Master Mix-Plus, template, and DEPC water. The melting curve was observed at 60 and 95 °C.[13]

Histological Studies. The brain was dissected, fixed in Bouin solution for 24 h, processed through a graded ethanol series, and embedded in paraffin for histological examination. For light microscopic analysis, the paraffin sections were sliced into 5-μm-thick slices and stained with hematoxylin and eosin.[24] Next, the sections were examined and captured on camera.

Pathomorphological Observation of Brain Edema by Thiomersal Administration. Four rats from each group were first injected with a thiomersal injection of 30 μg/mL dissolved in saline solution. After decapitating the rats, the brains were collected and fixed in 150 mL of 4% paraformaldehyde solution. Following routine paraffin embedding, each brain was sliced and stained with H&E. Each stained tissue section was photographed and examined under a light microscope.

Statistical Analysis. The variance (ANOVA) single factor test analysis was used for statistical analysis, with significance set at $p < 0.05$.

***In Silico* Study.** *Ligand Preparation.* The 2D structures of THIM and ascorbic acid (vitamin C) were obtained from the PubChem database (PubChem CID: 16684434 and 54670076).[25] All the sketched two-dimensional (2D) structures were transformed into 3D and geometry optimized by using Avogadro 1.2.0 software.[26] Geometry optimization has occurred to find the most stable conformers of all of the molecules. The results were saved in a separate folder in the PDB format.

Receptor Preparation. The 2D X-ray crystal structures of the following proteins were obtained from the RCSB Protein Data Bank (https://www.rcsb.org/) and prepared as receptors for molecular docking: MT-1 (PDB ID: Q53Z83), MT-2 (PDB ID: 4mt2), and MT-3 (PDB ID: P37361). The crystal structures were prepared by removing heteroatoms, water, and ions. Hydrogens were added, and missing residues were built using AutoDock Tools 1.5.7. The prepared structures were saved as PDBQT files.[27,28]

Molecular Docking. The software AutoDock 1.5.2 software was utilized to perform all molecular docking calculations. The PDBQT file of receptors was prepared using the AutoDock protocol. The maximum number of energy evaluations (evals) and the genetic algorithm number (GA) were changed to 250 and 25,000,000, respectively. The default settings for every other option were retained. The active sites were defined by the docking grid's dimensions.[28]

https://doi.org/10.1021/acsomega.3c07239
ACS Omega XXXX, XXX, XXX−XXX

Table 3. Blood Lipid Profile Analysis of Different Concentrations of Thiomersal[a]

parameters (mg/dL)	NC	group 1	group 2	group 3	group 4
TC	79 ± 2.21	135.1 ± 5.1	159.4 ± 3.21[c]	118 ± 3.7[c]	81 ± 2.9
TG	68.4 ± 2.31	115.3 ± 3.97	129.2 ± 2.1[c]	98.1 ± 2.3[c]	86.4 ± 2.1
HDL	60.5 ± 3.62	47.1 ± 2.1	38 ± 4.85[c]	46.4 ± 3.6[c]	58.1. ± 3.4
LDL	54 ± 2.33[c]	93.3 ± 5.9[c]	146.3 ± 3.66[c]	73.1 + 2.8[c]	63.4 ± 1.6[b]
VLDL	16.8 ± 2.73[c]	23.4 ± 4.1[c]	29.3 ± 3.97[c]	19.3 ± 1.09[b]	16.8 ± 1[b]

[a]NC, normal control; group 1: thiomersal (25 μg/mL); group 2: thiomersal (50 μg/mL); group 3: thiomersal (50 μg/mL) with vitamin C (5 μg/mL); group 4: vitamin C (5 μg/mL). [b]$p < 0.01$. [c]$p < 0.05$.

Table 4. Changes in Oxidative Stress Markers (SOD, CAT, GSH, TBARS, and NO) in the Serum, Liver, and Heart[e,f,g,j]

parameters		NC	group 1	group 2	group 3	group 4
serum	SOD[a]	37.1 ± 1.14	18.2 ± 2[++]	15.5 ± 3.6	28.6 ± 2.6[++]	39.6 ± 4.5
	GSH[b]	133 ± 4.5	209 ± 5.7	233 ± 3.1	175 ± 6.5	121 ± 1.6
	TBARS[c]	22.2 ± 1.1	49.8 ± 4.1	56.3 ± 3.81	37.3 ± 2.1	21.23 ± 2.2
	NO[d]	26.12 ± 1.32	58.4 ± 1.36	67.91 ± 1.51	45.31 ± 3.1	25.23 ± 2.6
liver	SOD[a]	85 ± 1.3	58 ± 1.2[+]	50.7 ± 1.4	64 ± 1.3[i]	79 ± 1.2
	GSH[b]	342 ± 8.6	279 ± 6.1	249 ± 5.7	289 ± 6.4	329 ± 4.4
	TBARS[c]	94.4 ± 5.2	169 ± 7.6[++]	177 ± 8.39	119.2 ± 7.4[i]	92 ± 5.6
	NO[d]	25.3 ± 2.3	47.2 ± 2.1	57.1 ± 3.4	44.3 ± 0.6	24.2 ± 2.1
heart	SOD[a]	66.4 ± 3.6	39.1 ± 1.4[+]	31.1 ± 2.5	49.1 ± 1.31[h]	59.2 ± 1.5
	GSH[b]	127 ± 4.3	88 ± 3.4[++]	75 ± 4.3	107 ± 6.4***	119 ± 2.3[h]
	TBARS[c]	37.2 ± 1.4	63.4 ± 4.3	71.1 ± 2.1	59 ± 2.1	34.1 ± 3.2
	NO[d]	18.1 ± 1.3	26.2 ± 1.4	29.16 ± 2.2	22.12 ± 1.1	17.14 ± 1.6

[a]% Inhibition. [b]μg/mg. [c]μM/mg. [d]μM/mg. [e]μg/mL. [f]μM/mL. [g]μM/mL. [h]$p < 0.05$ *vs* control. [i]$p < 0.01$ *vs* control, $n = 5$, mean ± SEM. [j]NC, normal control; group 1: thiomersal (25 μg/mL); group 2: thiomersal (50 μg/mL); group 3: thiomersal (50 μg/mL) with vitamin C (5 μg/mL); group 4: vitamin C (5 μg/mL).

RESULTS AND DISCUSSION

Effects of Vitamin C Therapy on Body Weight Gain. In this work, the body weights of rats administered different concentrations of thiomersal and vitamin C are displayed in Table 2. In thiomersal-treated rats, the data revealed a significant reduction in body weight as compared to the nontreated rats (control group). However, with vitamin C supply, the body weight became significantly greater than in rats exposed to thiomersal ($p < 0.05$).

Biochemical Parameters. *Blood Lipid Profile Analysis.* Table 3 demonstrates that the HCF group's serum lipid levels (TC, TG, VLDL-C, and LDL-C) were significantly higher than the NC group's ($p < 0.05$). Treatment was done with two different dose levels of thiomersal (25 μg/mL) in group 1 and thiomersal (50 μg/mL) in group 2. In groups 1 and 2, significantly increased plasma total cholesterol (TC) was 135 and 159, respectively, which represent 41 and 50 excesses in total cholesterol concentration. As a result of the vitamin administered with thiomersal, as shown in the group, the percentage of total cholesterol increased by 33%. In group 4, which represents the administered rats with vitamin C only, the total cholesterol is similar to the normal control group. Similarly, triglyceride (TG) results are likely the same as the total cholesterol result. Groups 1 and 2 showed small increases in the concentration of TG due to the administration of the rat's diet with vitamin C only. In the HDL shown in the verse process, the concentration of the mentioned parameters revealed a decreased value in groups 1, 2, 3, and 4, with concentrations of 21, 36, 23, and 3%, respectively. The HDL value increased by a factor of 41, 63, 19, and 14 for groups 1, 2, 3, and 4, respectively. Finally, the VLDL value showed an increase for groups 1, 2, 3, and 4 with percents of 30, 44, and 15, respectively. In group 4, which represents the administered rats with vitamin C only, the VLDL value is approximately the same as the normal control.

Oxidative Stress Parameter. The administration of thiomersal caused a significant adverse effect on the oxidative stress redox status. The data of oxidative stress markers, SOD, glutathione reductase, and NO, as displayed in Table 4, decreased the antioxidant parameters such as SOD, while GSH, TABRS, and NO showed an increase in their values after the administration of thiomersal for the samples collected from serum, heart, and liver. Because thiomersal is associated with vitamin C, the results of SOD were improved due to vitamin C's antioxidant effect. However, GSH, TABRS, and NO, as shown in Table 4, revealed a decrease in their values after the administration of the thiomersal combination with vitamin C. The results emphasized the amelioration effect of vitamin C as an antioxidant material.

Quantitative Reverse Transcriptase-Polymerase Chain Reaction. As shown in Figure 1A, the expressions of MT mRNAs in the cerebrum and cerebellum were observed for 6 h. The dose-dependent injection of THIM, The expression of MT-1 mRNA was significantly higher in the cerebellum but not in the cerebrum, when group 3 (50 μg/kg THIM was injected), and the expression was about 15-fold higher than that of the control group. The vitamin C attenuates the effect of the THIM on both the cerebrum and cerebellum in group 5 (50 μg/mL thiomersal associated with 5 μg/mL of vitamin C). Similarly, MT-2 mRNA significantly increased in both the cerebrum and cerebellum after 50 μg/kg THIM was injected; however, the expression of both tissues was about twofold higher than that of the control group. The vitamin C attenuate the effect of the THIM on both the cerebrum and cerebellum in group 5 (50 μg/mL thiomersal associated with 5 μg/mL of vitamin) as compared with group 3 (50 μg/kg THIM was

https://doi.org/10.1021/acsomega.3c07239
ACS Omega XXXX, XXX, XXX−XXX

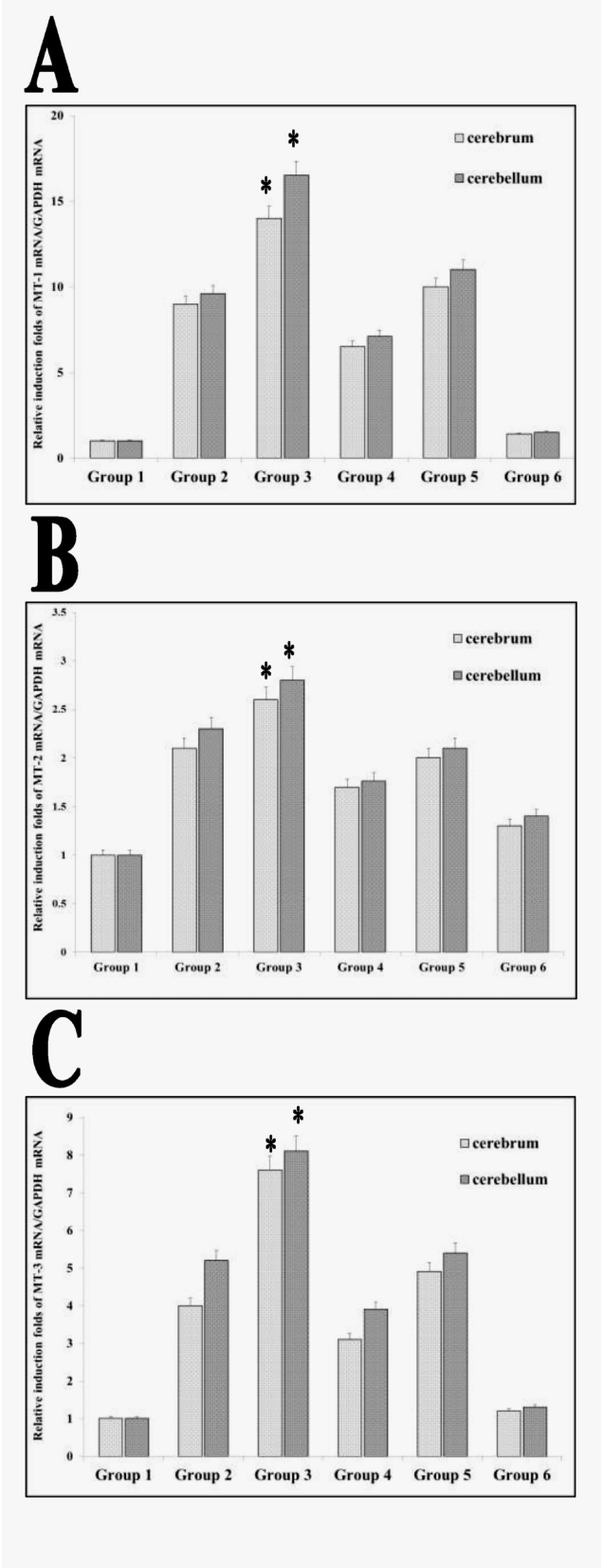

Figure 1. RT-PCR expression of the metallothionein (MT). (a) The expression relation of MT-1 Group 1: negative control (nontreated animal). Group 2: animal treated with 25 μg/mL of thiomersal. Group 3: animal treated with 50 μg/mL of thiomersal. Group 4: animal treated with 25 μg/mL of thiomersal associated with 5 μg/mL of vitamin C. Group 5: animal treated with 50 μg/mL of thiomersal associated with 5 μg/mL of vitamin C. Group 6: animal treated with 5 μg/mL of vitamin C only. (b) The expression relation of MT-2. Group 1: negative control (nontreated animal). Group 2: animal treated with 25 μg/mL of thiomersal. Group 3: animal treated with 50 μg/mL of thiomersal. Group 4: animal treated with 25 μg/mL of thiomersal associated with 5 μg/mL of vitamin C. Group 5: animal treated with 50 μg/mL of thiomersal associated with 5 μg/mL of vitamin C. Group 6: animal treated with 5 μg/mL of vitamin C only. (c) The expression relation of MT-3. Group 1: negative control (nontreated animal). Group 2: animal treated with 25 μg/mL of thiomersal. Group 3: animal treated with 50 μg/mL of thiomersal. Group 4: animal treated with 25 μg/mL of thiomersal associated with 5 μg/mL of vitamin C. Group 5: animal treated with 50 μg/mL of thiomersal associated with 5 μg/mL of vitamin C. Group 6: animal treated with 5 μg/mL of vitamin C only.

injected), as shown in Figure 1B. MT-3 mRNA significantly increased in the cerebellum when 25 or 50 μg/mL THIM was injected and was fivefold and eightfold higher than that of the control, respectively. The vitamin C decreased the effect of the THIM in both the cerebrum and cerebellum in group 5, which is 50 μg/mL thiomersal associated with 5 μg/mL of vitamin as compared with group 3 (50 μg/kg THIM was injected; Figure 1C). Finally, vitamin C decreased the adverse effect on both the cerebrum and cerebellum through decreases in the expression of metallothionein (MT).

Histological Results. Liver Tissue Section. Histopathological observation of the hepatic tissue of animals in the control group revealed the normal morphology of the liver cells, with average central veins (CV) and average hepatocytes arranged in single-cell cords with average intervening blood sinusoids, as shown in Figure 2A. Group 2 revealed that the existence of an expanded portal tract with surrounding hepatocytes showed apoptosis, binucleation, and karyomegaly, as displayed in Figure 2B. Figure 2C displays apoptotic hepatocytes with areas of necrosis and hemorrhage. As ascorbic acid was administered only, as Figure 2D shows, markedly dilated CV with congested blood sinusoids were revealed. Finally, the hepatic tissue, as shown by the association of ascorbic acid with thiomersal in Figure 2E, showed mildly expanded portal tracts with few hepatocytes showing karyomegaly and binucleation.

Brian Tissue Section. Histopathological observation of the cerebellar cortex of animals in the control group revealed a normal morphology of the cerebellar cortical cells and layers, as Figure 3A displays. Group 2 revealed that the separation of the Purkinje cells was due to the degeneration of Purkinje cells, and the granular layer degenerated stallate cells in the cerebellum, as Figure 3B revealed. Figure 3C shows degeneration and necrosis of the Purkinje cells of the cerebellar cortex in group 3. While the results of animal cerebellar cortices observations in group 3, little degeneration of Purkinje cells of the cerebellum was observed, with clumping and congestion of cells. It was also noticed that there was a markedly congested blood vessel with marked edema and an area of hemorrhage and astrogliosis, as displayed in Figure 3C. The cerebellar cortex of animals showed displacement of Purkinje cell nuclei; separation of Purkinje cells due to the degeneration of Purkinje cells, but the granular and molecular layers of the cerebellum were not affected, as shown in Figure 3D. Finally, the cerebellar cortex of animals in group 4 revealed a normal arrangement of the layers and cells of the cerebellum, as shown in Figure 3E.

https://doi.org/10.1021/acsomega.3c07239
ACS Omega XXXX, XXX, XXX−XXX

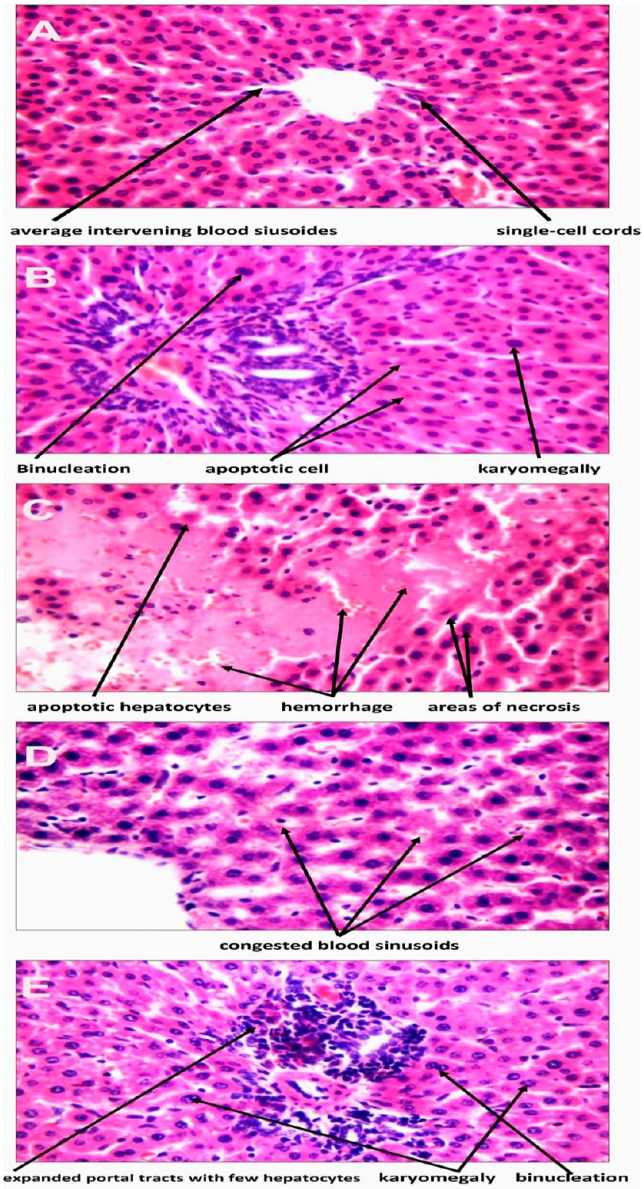

Figure 2. Histopathological study of hepatic tissue after thiomersal administration of the liver tissue of the animals. (a) Group 1: negative control (nontreated animal). (b) Group 2: animal treated with 25 μg/mL of thiomersal. (c) Group 3: animal treated with 50 μg/mL of thiomersal. (d) Group 4: animal treated with 25 μg/mL of thiomersal associated with 5 μg/mL of vitamin C. (e) Group 5: animal treated with 50 μg/mL of thiomersal associated with 5 μg/mL of vitamin C. (f) Group 6: animal treated with 5 μg/mL of vitamin C only.

Morphological Features of Brain Edema Following Thiomersal Administration. No abnormal changes were observed in the control group (Figure 4A). As Figure 4B shows, after 6 h of TBI, a light-colored edema zone occurred in the contusion penumbra (CP), whereas larger gaps between

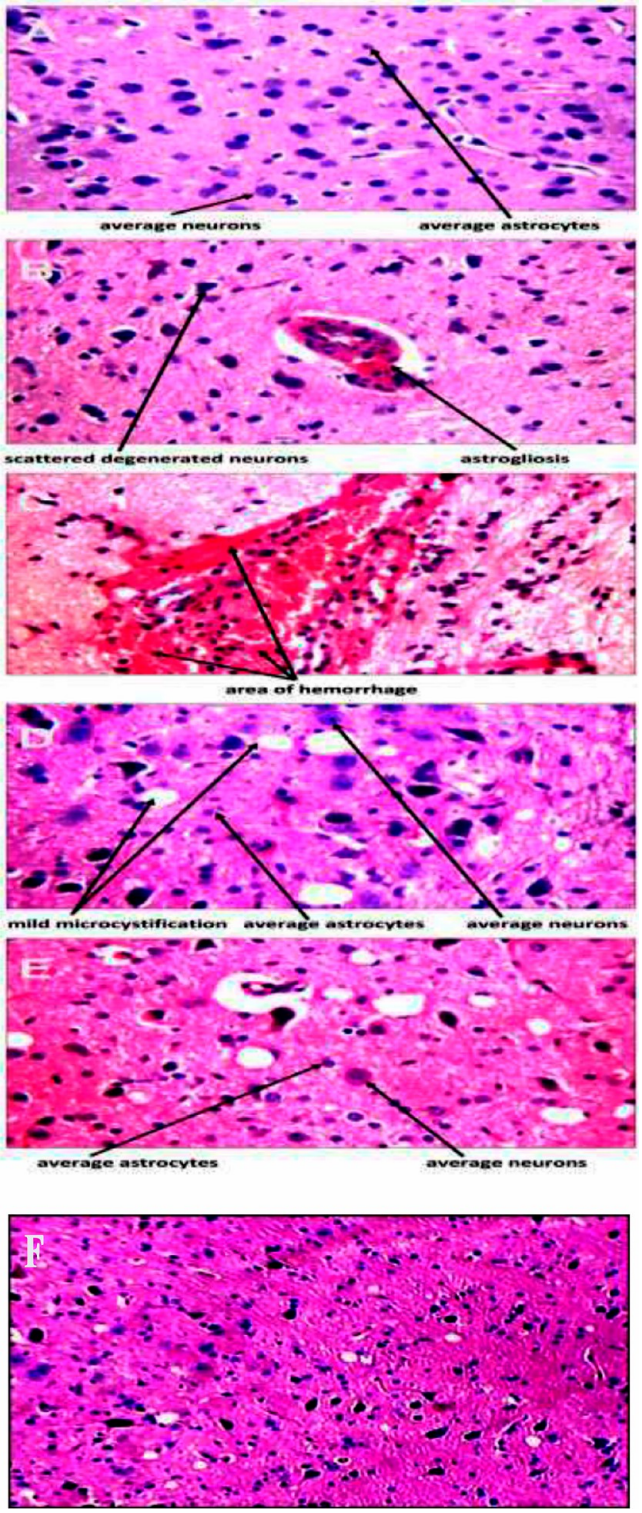

Figure 3. Histopathological study of the brain following thiomersal administration of the cerebellar cortex of animals. (a) Group 1: negative control (nontreated animal). (b) Group 2: animal treated with 25 μg/mL of thiomersal. (c) Group 3: animal treated with 50 μg/mL of thiomersal. (d) Group 4: animal treated with 25 μg/mL of thiomersal associated with 5 μg/mL of vitamin C. (e) Group 5: animal treated with 50 μg/mL of thiomersal associated with 5 μg/mL of vitamin C. (f) Group 6: animal treated with 5 μg/mL of vitamin C only.

https://doi.org/10.1021/acsomega.3c07239
ACS Omega XXXX, XXX, XXX−XXX

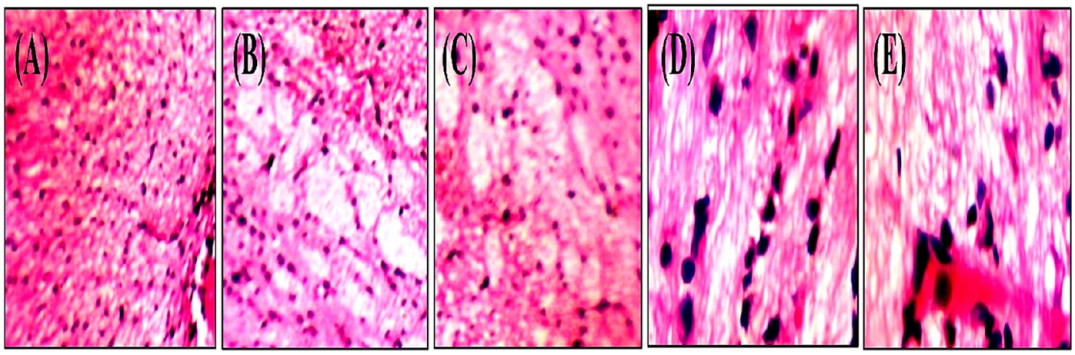

Figure 4. Morphological features of brain edema following thiomersal administration. (a) Control group (nontreated). (b) At 6 h after TBI. (c) After 12 h of TBI. (d) After 24 h of TBI. (e) After 48 h of TBI.

Table 5. Interaction of Vitamin C and Thimerosal with Metallothionein Isoforms (MT-1, MT-2, and MT-3)

Compound	Protein	ΔG (kcal/mol)	2D	Interactions
Vitamin C	MT-1	-4.4	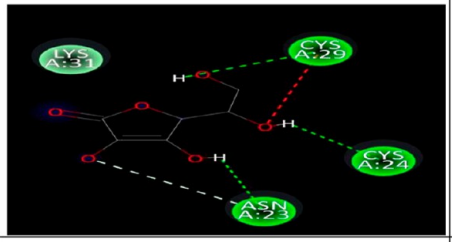	H- Bond: (CYS 29, CYS 24, ASN 23): Van der Waals bond : LYS 31 Carbon hydrogen Bond: ASN 23 Unfavorable Acceptor–Acceptor: (CYS 29)
Vitamin C	MT-2	-4.9	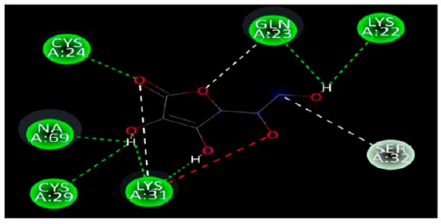	H- Bond: (LYS 22, LYS 31, GLN 23, CYC 24, NA 69, CYS 29),Carbon hydrogen Bond: (Ser 32, GLN 23 and LYS 31) Unfavorable Acceptor–Acceptor: (LYS 31)
Vitamin C	MT-3	-4.4	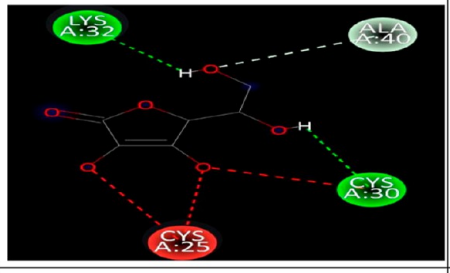	H Bond : (LYS 32 , CYS 30) Carbon hydrogen Bond: (ALA 40) and Unfavor Acceptor-Acceptor (CYS 25, CYS 30)
Thimerosal	MT-2	-4.1	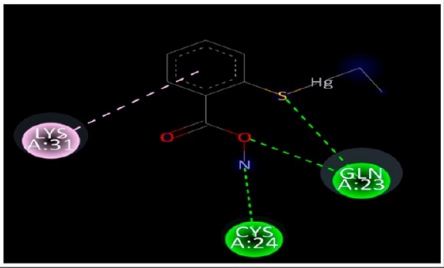	H- Bond: (CYS 24, 2GLN23) Pi- Alkyl bond: (LYS 31)

blood vessels were observed, indicating vasogenic edema. After 12 h of TBI, as Figure 4C displays, there is intracellular vacuolar degeneration with a narrowing of the intercellular spaces. As Figure 4D shows, after 24 h of TBI, intracellular edema and vasogenic edema were aggravated, whereas large areas of vacuole-like cells and a light-colored latticed intercellular substance were observed. After 48 h of TBI, as Figure 4E revealed, intracellular edema and vasogenic edema were alleviated, but vasogenic edema was aggravated again.

In Silico Study. Molecular docking simulation studies were performed between vitamin C compounds and the binding pocket of metallothionein isoforms (MT-1, MT-2, and MT-3)

https://doi.org/10.1021/acsomega.3c07239
ACS Omega XXXX, XXX, XXX−XXX

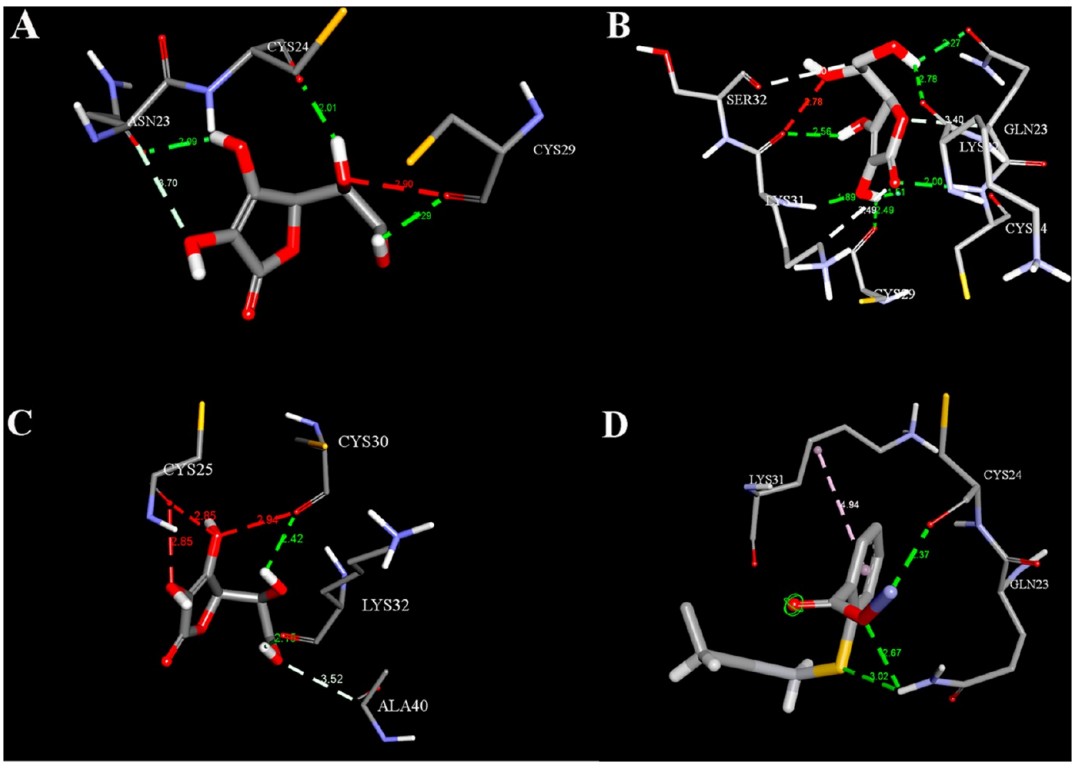

Figure 5. (A) 3-D structure of molecular docking between vitamin C and MT-1 (PDB ID: P37361). (B) 3-D structure of molecular docking between vitamin C and MT-2 (PDB ID: 4mt2). (C) 3-D structure of molecular docking between vitamin C and MT-3 (PDB ID: P37361). (D) 3-D structure of molecular docking between THIM and MT-2 (PDB ID: 4mt2).

protein receptors of Rattus model MT-1 (PDB ID: Q53Z83), MT-2 (PDB ID: 4mt2), and MT-3 (PDB ID: P37361). Table 5 summarizes the binding energy of vitamin C interacting with the catalytic site in the protein of Rattus MT-1 (PDB ID: Q53Z83), which reveals that the binding affinity of the protein with vitamin C occurred via the H-bond (Cys 24, Cys 29, and Ans 23) with ΔG = −4.4 kcal/mol. Similarly, the docking analysis displayed the best-docked conformation of vitamin C and MT-2 (PDB ID: 4mt2). The binding energy with the best-chosen pose was −4.9 kcal/mol. The 2D analysis of the active site revealed the presence of van der Waals forces between the ligand and one protein residue Ser 32, six hydrogen bonds with Lys 22, Lys 31, Gln23, Cyc 24, Cyc 29, and NA 69, and the unfavorable acceptor−acceptor bond Lys 31. The docking analysis of vitamin C and MT-3 (PDB ID: P37361), the binding energy of the best-selected pose was −4.4 kcal/mol. The 2D analysis of the active site showed the involvement of van der Waals forces between the ligand and one residue from the protein with Aln 40 and two H-bonds (Cys 30 and Lys 32) and unfavorable interactions between Cys 25 and vitamin C. While their interaction with MT-2 (PDB ID: 4mt2) had a binding energy of −4.1 kcal/mol, the active site's 2D analysis revealed the presence of van der Waals forces between the ligand and seven protein residues, (Cys 33, Ser 32, NA 69, Lys 22, Lys 25, Lys 30, Val 39), and four residue interactions with the ligand via H-bond (Cys 24, 2Gln 23, Cys 24, Asn 23), and one residue by pi-alkyl bond (LYS 31). The 3-D analysis of the active site showed the distance between MT-1 (PDB ID: Q53Z83) and vitamin C, as shown in Figure 5A, A where Cys 24 and Cys 29 were bound to the vitamin with hydrogen bonds of 2.01 and 2.29 Å, respectively. Also, Asn 23 was bound to vitamin C with two different bonds: a hydrogen bond with a length of 2.09 μm and a carbon bond with a length of 3.7 μm. Similarly, vitamin C was bound to MT-2 (PDB ID: 4MT2) via two hydrogen bonds to Gln 23 with bond lengths of 2.27 and 2.78 Å. Also, Lys 31 was bound to vitamin C via an H-bond with a length of 2.49, 1.51, and 1.89 A, and one C-bond with a length of 2.49 A. Ser 32 was bound to vit-C by one H-bond and one C-bond with lengths of 2.56 and 3.5 Å, respectively. MT-3 (PDB ID: P37361) was bound to Vit-C as shown in Figure 5C by one H-bond between Vit-C and Cys 30 and one H-bond with Lys 32 and Vit-C with bond lengths of 2.42 and 2.15 Å, respectively. Finally, THIM has interacted with MT-2 (PBD ID: 4MT2) with three H-bonds and one C-bond as follows: one H-bond with Cys24 with a length of 2.37 Å, two H-bonds with Gln 23 with bond lengths of 2.67 and 3.02 Å, and a C-bond with Lys 31 with a C-bond of 4.94 Å (Figure 5B).

DISCUSSION

The accumulation of heavy metals inside organs, such as the liver, kidney, and brain, causes adverse effects on their function and morphology. Also, it contributes to high metabolic activity. Lead, mercury, and antimony levels were higher in the gills than in the liver and the other two tissues (muscle and blood).[29] THIM increase in apoptotic cells in the prefrontal cortex of premature rats leads to impairment of learning.[30,31] THIM was dismantled from the vaccine's use in developed countries due to its adverse effects, while it is still used in low- and middle-income countries.[32] THIM causes various neurotoxic alterations in microglia and astrocytes. A previous report has shown that THIM concentrations ranging from 0.16 to 10 μM can cause cell death in cultured human cortical neurons.[33,34] The combination of heavy metals such as lead

https://doi.org/10.1021/acsomega.3c07239
ACS Omega XXXX, XXX, XXX−XXX

and mercury causes synergistic effects.[35] Potentially, the existence of mercury in the brain can activate the brain's neuroinflammatory response to a peripheral or central immune trigger.[36] The brain's immune response lowers GSH levels, which can cause microglia-mediated neurotoxicity,[36] and alters NF-κB functioning, which can produce chronic or excessive neuroinflammation.[6,10] Interestingly, vitamin C has a central role in regenerating oxidized vitamin E and recovering the antioxidant activity of vitamin E.[37] Ebuehi *et al.*[40] demonstrated that associated vitamins C and E significantly decrease the blood lead concentration and attenuate hepatic tissue damage with a significant reduction in oxidative stress in the brain tissues of rats.[38,39] Also, the association of the thiomersal with vitamin C may lead to chelating heavy metals and discarding them from the body. Therefore, it improved the body weight. During the study, there was a significant excess of LPO during therimosal admission due to the formation of free radicals that lead to increased oxidative stress and the accumulation of heavy metals such as ethylmercury that are involved in thiomersal. There is a tremendous deficiency in antioxidant enzymes, such as SOD and glutathione reductase. The deficiency of the antioxidant system is due to an increase in the concentration of mercury, which leads to the unequalization of the pro-antioxidant balance in the body.[40] However, as vitamin C was associated with the therimosal, the antioxidant enzymes were increased due to the ability of vitamin C to chelate the ethylmercury of the therimosal. The administration of high doses of thiomersal without vitamin C caused the degeneration and necrosis of Purkinje cells in the Purkinje cell layers of the cerebellum in Wistar albino rats compared with the normal control. As Giularte reported, most heavy metals are capable of damaging the nervous system as well as liver cells. Interestingly, as Rapoport and Schweizer reported, the most sensitive part of the cerebellar cortex is the Purkinje cells. Verina *et al.* mentioned that the Purkinje cells can interact with noxious substances through degeneration and disappearance from relative positions in the Purkinje cell layer.[41,42] MT-1 and MT-2 are acute-phase proteins that are activated in both astrocytes and microglia by several stimuli, including mercury compounds, and play a vital role in protecting the central nervous system from damage by activating the following antioxidative, anti-inflammatory, neurodegenerative, and apoptotic behaviors in the brain.[43] Also, MT promotes neuronal differentiation and has neuroprotective properties. However, the previous reports stated that MT-3 is initially expressed in neurons, but MT-3 is also known to be expressed in astrocytes.[44] The lower binding energy (ΔG) indicates a stronger binding affinity for the ligand to the protein target. In this case, vitamin C has a lower ΔG of −4.8 kcal/mol compared to −4.1 kcal/mol for THIM, suggesting that vitamin C binds more favorably to MT-2. The 2D ligand−protein interaction diagrams provide insights into specific binding modes. Vitamin C forms multiple hydrogen bonds with key MT residues Lys31, Gln23, Cys24, Cys29, and the sodium ion. It also exhibits carbon−hydrogen bonding with Ser32 and Gln23.[45] The multiple hydrogen bonds formed between vitamin C and MT residues Lys31, Gln23, Cys24, and Cys29 and the sodium ion represent key stabilizing interactions. Hydrogen bonds involve electrostatic interactions between hydrogen atom donors (*e.g.*, hydroxyl groups) and acceptors (*e.g.*, carbonyl oxygens). The distances between heavy atoms are typically 2.5−3.5 Å. H-bonds provide directed high-affinity interactions to anchor the ligand in the binding site. The five hydrogen bonds formed by vitamin C allow it to form a stable complex with MT. his extensive H-bonding network anchors vitamin C firmly in the MT binding pocket. However, THIM forms only two H-bonds to Gln23 and Cys24. This provides less stabilization in the binding pocket, contributing to the lower affinity compared to vitamin C. Structural modifications to introduce additional H-bonding functional groups could improve THIM binding. The alkyl moiety in thiomersal forms hydrophobic contacts with Lys31. Such hydrophobic interactions contribute to binding affinity but are less directional than H-bonds. Vitamin C does not have alkyl groups to form hydrophobic contacts. The alkyl moiety in thiomersal forms hydrophobic contacts with Lys31. Such hydrophobic interactions contribute to binding affinity but are less directional than H-bonds. Vitamin C does not have alkyl groups to form hydrophobic contacts. The extensive H-bonding network formed by vitamin C allows high affinity, guided interactions for optimal fit in the MT binding site. Incorporating H-bond donors and acceptors into THIM could significantly improve its binding through similar strong, directed interactions with MT residues.[45] Previous studies mentioned that cerebellar neurodegeneration leads to lesions of the cerebellum, which are indicated by signs and symptoms generally called "cerebellar syndromes" that involve muscular hypotonia, intentional tremor, nystagmus, scanning speech, and ataxic gait.[46] Brain edema is classified into two types: vasogenic and intracellular.[47] Vasogenic edema is caused by the passage of water and plasma proteins into the interstitial space as a result of a BBB defect.[48] After an excessive water influx into cells, intracellular edema occurred as a result of mitochondrial swelling, which disrupted ATP generation. Furthermore, a decreased cerebral blood flow impairs ion movement and exacerbates intracellular edema. In general, the edema cycle continues until death. Also, it can cause a permanent injury.[49] Previous studies reported that the pathological changes in the center of trauma were caused by vasogenic edema.[32,49−51] In the present work, vitamin C has an ameliorative effect on reducing neurotoxicity in the cerebellum induced by thiomersal by increasing the levels of antioxidants and decreasing the levels of expression of MT-1, MT-2, and MT-3. Also, it decreases the apoptotic cells in both hepatic and brain cells. Finally, vitamin C plays a central role in attenuating the severe effects of heavy metals in different organs throughout the body.

CONCLUSIONS

In this study, the administration of THIM in various doses was investigated in the presence or absence of vitamin C. The experiments were carried out by blood lipid profile analysis, an oxidative stress assay, and the histopathology of the cerebral cortex in Wistar albino rats. The data showed that an excess of THIM caused an antioxidant system dysfunction. Also, there are increases in oxidative stress and blood lipid profiles due to the existence of free radicals as a result of the acculturation of lead metal inside the organs. In contrast, the results were changed to be better because of vitamin C associated with THIM. The computation studies showed that vitamin C has a lower ΔG of −4.9 kcal/mol compared to −4.1 kcal/mol for THIM to bind to MT-2 protein, which demonstrated the ability of vitamin C to bind toward MT-2 than THIM. The extensive H-bonding network formed by vitamin C allows high-affinity, guided interactions for an optimal fit in the MT binding site. The histopathological observations in liver tissues

https://doi.org/10.1021/acsomega.3c07239
ACS Omega XXXX, XXX, XXX−XXX

showed an association of ascorbic acid with thiomersal and mildly expanded portal tracts, with a few hepatocytes showing karyomegaly and binucleation. The histopathological observations in the brain tissue section displayed that the cerebellum has degenerative, necrotic, and cerebellar neurodegeneration, which leads to lesions in the cerebellum. Also, the vasogenic edema increased as the concentration of THIM increased. It indicated that the presence of vitamin C decreased the neurotoxicity of THIM.

■ ASSOCIATED CONTENT

Data Availability Statement

The original contributions presented in the study are included in the article Material; further inquiries can be directed to the corresponding author.

■ AUTHOR INFORMATION

Corresponding Author

Amr Hassan − *Department of Bioinformatics, Genetic Engineering and Biotechnology Research Institute (GEBRI), University of Sadat City, Sadat 32897, Egypt;* orcid.org/0000-0001-6623-2179;
Email: amrhassan.nanotechnology@gmail.com

Authors

Reham Mohsen − *College of Biotechnology, October University for Modern Science and Arts (MSA), University Giza, Giza 11456, Egypt*

Ahmed Rezk − *College of Biotechnology, October University for Modern Science and Arts (MSA), University Giza, Giza 11456, Egypt*

Gabrielle Bangay − *CBIOS—Research Center for Biosciences & Health Technologies, Universidade Lusófona de Humanidades e Tecnologias, Lisboa 1749-024, Portugal; Facultad de Farmacia, Departamento de Ciencias Biomédicas (Área de Farmacología; Nuevos agentes antitumorales, Acción tóxica sobre células leucémicas), Universidad de Alcalá de Henares, Alcalá de Henares 600 28805 Madrid, Espana*

Patrícia Rijo − *CBIOS—Research Center for Biosciences & Health Technologies, Universidade Lusófona de Humanidades e Tecnologias, Lisboa 1749-024, Portugal; Instituto de Investigação do Medicamento (iMed.ULisboa), Faculdade de Farmácia, Universidade de Lisboa, Lisbon 1749-024, Portugal;* orcid.org/0000-0001-7992-8343

Mona F. M. Soliman − *Department of Histology and Cell Biology, Faculty Medicine, Mansoura University, Mansoura 35516, Egypt*

Mohamed G. A. Hablas − *Department of Histology and Cell Biology, Faculty of Medicine, Suez University, Suez 43221, Egypt*

Khalifa AbdulRazik K. Swidan − *Department of Histology and Cell Biology, Faculty of Medicine, Suez University, Suez 43221, Egypt*

Tahseen S. Mohammed − *Department of Public Health and Community Medicine, Faculty of Medicine, Al-Azhar University, Cairo 11884, Egypt*

Mohammad A. Zoair − *Department of Physiology, Faculty of Medicine, Al-Azhar University, Cairo 11884, Egypt*

Abir A. Khalil Mohamed − *Department of Zoology, Faculty of Science, Girls Branch, Al-Azhar University, Cairo 11884, Egypt*

Tamer I. Abdalrhman − *Department of Histology, Faculty of Medicine, Al-Azhar University, Assiut 71524, Egypt*

Ahmad M. Abdel-aleem Desoky − *Department of Histology, Faculty of Medicine, Al-Azhar University, Assiut 71524, Egypt*

Dalia D. Mohamed − *Department of Industrial Biotechnology, Genetic Engineering and Biotechnology Research Institute (GEBRI), University of Sadat City, Sadat 32897, Egypt*

Doaa D. Mohamed − *Department of Industrial Biotechnology, Genetic Engineering and Biotechnology Research Institute (GEBRI), University of Sadat City, Sadat 32897, Egypt*

Ahmed I. Abd El Maksoud − *Department of Industrial Biotechnology, Genetic Engineering and Biotechnology Research Institute (GEBRI), University of Sadat City, Sadat 32897, Egypt*

Aly F. Mohamed − *Holding Company for Vaccine and Sera Production (VACSERA), Giza 22311, Egypt*

Complete contact information is available at: https://pubs.acs.org/10.1021/acsomega.3c07239

Author Contributions

A.H., R.M., and A.F.M. contributed to the conceptualization. A.H. and A.F.M. contributed to formal analysis. A.H. and A.F.M. contributed to funding acquisition. A.R., R.M., A.H., D.D.M., D.D.M., A.I., and A.E.M. contributed to investigation. R.M., A.F.M., A.R., and A.H. contributed to the Methodology. A.H. and A.I.A.E.M. contributed to Project administration.; A.I.A.E.M., R.M., G.B., P.R., M.G.A.H., K. A.K.S., and M.F.M.S., contributed to Resource allocation. A.H. contributed to Supervision. A.F.M., A.R., A.H., and A.I.A.E.M. contributed to Validation of data. A.F.M., A.R., A.H., and P.R. contributed to Visualization. A.I.A.E.M., T.I.A., A.M.A.D., A.F.M., G.B., P.R., and A.H. contributed to the writing original draft. A.H., A.I.A.E.M., A.F.M., G.B., and P.R. contributed to writing -review edition. All authors approved the final version of the manuscript.

Notes

The authors declare no competing financial interest.
Ethics statement. We followed the entire Council Directive of the European Communities (Directive 2010/63/EU of September 22, 2010). According to the Institutional Animal Care and Use Committee with oversight of the faculty of Veterinary Medicine, University of Sadat City, Sadat City, Egypt (Ethical approval number: VUSC-043-1-22).

■ ACKNOWLEDGMENTS

The authors would like to thank to Fundação para a Ciência e Tecnologia (FCT) with the references DOI: 10.54499/UIDP/04567/2020 and DOI: 10.54499/UIDB/04567/2020 from Portugal. Also, the authors were thankful for Dr. Amr Hassan and Dr. Ahmed G. Soliman and it research Centre I-Mole for its docking facilities.

■ REFERENCES

(1) Geier, D. A.; King, P. G.; Hooker, B. S.; Dórea, J. G.; Kern, J. K.; Sykes, L. K.; Geier, M. R. Thimerosal: clinical, epidemiologic and biochemical studies. *Clin. Chim. Acta* **2015**, *444*, 212−220.

(2) Olczak, M.; Duszczyk, M.; Mierzejewski, P.; Bobrowicz, T.; Majewska, M. D. Neonatal administration of thimerosal causes persistent changes in mu opioid receptors in the rat brain. *Neurochem. Res.* **2010**, *35*, 1840−1847.

(3) Clarkson, T. W.; Magos, L.; Myers, G. J. The toxicology of mercury—current exposures and clinical manifestations. *N. Engl. J. Med.* **2003**, *349* (18), 1731−1737.

(4) Clifton, J. C., II Mercury exposure and public health. *Pediatr. Clin.* **2007**, *54* (2), 237.e1.
(5) Clarkson, T. W. The three modern faces of mercury. *Environ. Health Perspect.* **2002**, *110* (suppl 1), 11−23.
(6) Kern, J. K.; Geier, D. A.; Audhya, T.; King, P. G.; Sykes, L. K.; Geier, M. R. Evidence of parallels between mercury intoxication and the brain pathology in autism. *Acta Neurobiol. Exp.* **2012**, *72* (2), 113−153.
(7) Pichichero, M. E.; Gentile, A.; Giglio, N.; Umido, V.; Clarkson, T.; Cernichiari, E.; Zareba, G.; Gotelli, C.; Gotelli, M.; Yan, L.; et al. Mercury levels in newborns and infants after receipt of thimerosal-containing vaccines. *Pediatrics.* **2008**, *121* (2), e208−e214.
(8) Ceccatelli, S.; Daré, E.; Moors, M. Methylmercury-induced neurotoxicity and apoptosis. *Chem. Biol. Interact.* **2010**, *188* (2), 301−308.
(9) Aschner, M.; Onishchenko, N.; Ceccatelli, S. Toxicology of alkylmercury compounds. *Organometallics in Environment and Toxicology: Metal Ions in Life Sciences*; The Royal Society of Chemistry, 2010; Vol. 7, pp 403−434.
(10) Kern, J.; Geier, D.; Homme, K.; King, P.; Bjørklund, G.; Chirumbolo, S.; Geier, M. Developmental neurotoxicants and the vulnerable male brain: a systematic review of suspected neurotoxicants that disproportionally affect males. *Acta Neurobiol. Exp.* **2017**, *77* (4), 269−296.
(11) Nordberg, G. F.; Gerhardsson, L.; Mumtaz, M. M.; Ruiz, P.; Fowler, B. A. Interactions and mixtures in metal toxicology. *Handbook on the Toxicology of Metals*; Academic Press, 2022; pp 319−347.
(12) Minami, T.; Miyata, E.; Sakamoto, Y.; Yamazaki, H.; Ichida, S. Induction of metallothionein in mouse cerebellum and cerebrum with low-dose thimerosal injection. *Cell Biol. Toxicol.* **2010**, *26*, 143−152.
(13) Hassan, A.; Al-Salmi, F. A.; Saleh, M. A.; Sabatier, J. M.; Alatawi, F. A.; Alenezi, M. A.; Albalwe, F. M.; Albalawi, H. M. R.; Darwish, D. B. E.; Sharaf, E. M. Inhibition Mechanism of Methicillin-Resistant Staphylococcus aureus by Zinc Oxide Nanorods via Suppresses Penicillin-Binding Protein 2a. *ACS Omega* **2023**, *8* (11), 9969−9977.
(14) Corps, K. N.; Roth, T. L.; McGavern, D. B. Inflammation and Neuroprotection in Traumatic Brain Injury. *JAMA Neurol.* **2015**, *72* (3), 355−362.
(15) Ren, H.; Lu, H. Dynamic features of brain edema in rat models of traumatic brain injury. *Neuroreport.* **2019**, *30* (9), 605−611.
(16) Gupta, S.; Aggarwal, S.; Rashanravan, B.; Lee, T. Th1-and Th2-like cytokines in CD4+ and CD8+ T cells in autism. *J. Neuroimmunol.* **1998**, *85* (1), 106−109.
(17) Aysun, H. An overview of ascorbic acid biochemistry. *Journal of Faculty of Pharmacy of Ankara University.* **2009**, *38* (3), 233−255.
(18) Hassan, A.; Elebeedy, D.; Matar, E. R.; Fahmy Mohamed Elsayed, A.; Abd El Maksoud, A. I. Investigation of angiogenesis and wound healing potential mechanisms of zinc oxide nanorods. *Front. Pharmacol* **2021**, *12*, 661217.
(19) Friedewald, W. T.; Levy, R. I.; Fredrickson, D. S. Estimation of the concentration of low-density lipoprotein cholesterol in plasma, without use of the preparative ultracentrifuge. *Clin. Chem.* **1972**, *18* (6), 499−502.
(20) Hassan, A.; Rijo, P.; Abuamara, T. M. M.; et al. Synergistic Differential DNA Demethylation Activity of Danshensu (Salvia miltiorrhiza) Associated with Different Probiotics in Nonalcoholic Fatty Liver Disease. *Biomedicines* **2024**, *12*, 279.
(21) Hassan, A.; Al-Salmi, F. A.; Abuamara, T. M. M.; Matar, E. R.; Amer, M. E.; Fayed, E. M. M.; Hablas, M. G. A.; Mohammed, T. S.; Ali, H.; Abd EL-fattah, F. M.; et al. Ultrastructural analysis of zinc oxide nanospheres enhances anti-tumor efficacy against Hepatoma. *Front. Oncol.* **2022**, *12*, 933750.
(22) Marklund, S.; Marklund, G. Involvement of the superoxide anion radical in the autoxidation of pyrogallol and a convenient assay for superoxide dismutase. *Eur. J. Biochem.* **1974**, *47* (3), 469−474.
(23) Green, L. C.; Wagner, D. A.; Glogowski, J.; Skipper, P. L.; Wishnok, J. S.; Tannenbaum, S. R. Analysis of nitrate, nitrite, and [15N] nitrate in biological fluids. *Anal. Biochem.* **1982**, *126* (1), 131−138.
(24) Khalil, H.; Nada, A. H.; Mahrous, H.; Hassan, A.; Rijo, P.; Ibrahim, I. A.; Mohamed, D. D.; AL-Salmi, F. A.; Mohamed, D. D.; Elmaksoud, A. I. A. Amelioration effect of 18β-Glycyrrhetinic acid on methylation inhibitors in hepatocarcinogenesis -induced by diethylnitrosamine. *Front. Immunol.* **2024**, *14*, 1206990.
(25) Kim, S.; Chen, J.; Cheng, T.; Gindulyte, A.; He, J.; He, S.; Li, Q.; Shoemaker, B. A.; Thiessen, P. A.; Yu, B.; et al. PubChem in 2021: new data content and improved web interfaces. *Nucleic Acids Res.* **2021**, *49* (D1), D1388−D1395.
(26) Hanwell, M. D.; Curtis, D. E.; Lonie, D. C.; Vandermeersch, T.; Zurek, E.; Hutchison, G. R. Avogadro: an advanced semantic chemical editor, visualization, and analysis platform. *J. Cheminf.* **2012**, *4*, 17.
(27) Morris, G. M.; Huey, R.; Lindstrom, W.; Sanner, M. F.; Belew, R. K.; Goodsell, D. S.; Olson, A. J. AutoDock4 and AutoDockTools4: Automated docking with selective receptor flexibility. *J. Comput. Chem.* **2009**, *30* (16), 2785−2791.
(28) Zhang, Z.; Li, Y.; Lin, B.; Schroeder, M.; Huang, B. Identification of cavities on protein surface using multiple computational approaches for drug binding site prediction. *Bioinformatics* **2011**, *27* (15), 2083−2088.
(29) Jithesh, M.; Radhakrishnan, M. V. Seasonal variation in accumulation of metals in selected tissues of the Ribbon fish, Trichiurus lepturus collected from Chaliyar River, Kerala, India. *Journal of Entomology and Zoology Studies.* **2017**, *5* (1), 51−56.
(30) Navazani, P.; Vaseghi, S.; Hashemi, M.; Shafaati, M. R.; Nasehi, M. Effects of Treadmill Exercise on the Expression Level of BAX, BAD, BCL-2, BCL-XL, TFAM, and PGC-1α in the Hippocampus of Thimerosal-Treated Rats. *Neurotox. Res.* **2021**, *39* (4), 1274−1284.
(31) Kern, J. K.; Geier, D. A.; Homme, K. G.; Geier, M. R. Examining the evidence that ethylmercury crosses the blood-brain barrier. *Environ. Toxicol. Pharmacol.* **2020**, *74*, 103312.
(32) Pedrozo-Penafiel, M. J.; Miranda-Andrades, J. R.; Gutierrez-Beleño, L. M.; Larrudé, D. G.; Aucelio, R. Q. Indirect voltammetric determination of thiomersal in influenza vaccine using photo-degradation and graphene quantum dots modified glassy carbon electrode. *Talanta* **2020**, *215*, 120938.
(33) Yel, L.; Brown, L. E.; Su, K.; Gollapudi, S.; Gupta, S. Thimerosal induces neuronal cell apoptosis by causing cytochrome c and apoptosis-inducing factor release from mitochondria. *Int. J. Mol. Med.* **2005**, *16* (6), 971−977.
(34) Dórea, J. G. Integrating experimental (in vitro and in vivo) neurotoxicity studies of low-dose thimerosal relevant to vaccines. *Neurochem. Res.* **2011**, *36*, 927−938.
(35) Gómez-Oliván, L. M.; Mendoza-Zenil, Y. P.; SanJuan-Reyes, N.; Galar-Martínez, M.; Ramírez-Durán, N.; Rodríguez Martín-Doimeadios, R. d. C.; Rodríguez-Fariñas, N.; Islas-Flores, H.; Elizalde-Velázquez, A.; García-Medina, S.; et al. Geno-and cytotoxicity induced on Cyprinus carpio by aluminum, iron, mercury and mixture thereof. *Ecotoxicol. Environ. Saf.* **2017**, *135*, 98−105.
(36) Lee, R. H.; Mills, E. A.; Schwartz, N.; Bell, M. R.; Deeg, K. E.; Ruthazer, E. S.; Marsh-Armstrong, N.; Aizenman, C. D. Neuro-developmental effects of chronic exposure to elevated levels of pro-inflammatory cytokines in a developing visual system. *Neural Dev.* **2010**, *5* (1), 2.
(37) Geier, D. A.; Geier, M. R. A prospective study of mercury toxicity biomarkers in autistic spectrum disorders. *J. Toxicol. Environ. Health* **2007**, *70* (20), 1723−1730.
(38) Shahsavani, D.; Baghishani, H.; Nourian, K. Effect of thiamine and vitamin C on tissue lead accumulation following experimental lead poisoning in Cyprinus carpio. *Iranian Journal of Veterinary Science and Technology.* **2017**, *9* (1), 39−44.
(39) Sahiti, H.; Bislimi, K.; Rexhepi, A.; Dalo, E. Metal accumulation and effect of vitamin C and E in accumulated heavy metals in different tissues in common carp (Cyprinus carpio) treated with heavy metals. *Polym. J. Environ. Stud.* **2019**, *29* (1), 799−805.
(40) Ebuehi, O. A. T.; Ogedegbe, R. A.; Ebuehi, O. M. Oral Administration of Vitamin C and Vitamin E amelioratesLead-induced

https://doi.org/10.1021/acsomega.3c07239
ACS Omega XXXX, XXX, XXX−XXX

Hepatotoxicity and Oxidative Stress in the Rat Brain. *Niger. Q. J. Hosp. Med.* **2012**, *22* (2), 85−90.
(41) Verina, T.; Rohde, C. A.; Guilarte, T. R. Environmental lead exposure during early life alters granule cell neurogenesis and morphology in the hippocampus of young adult rats. *Neuroscience.* **2007**, *145* (3), 1037−1047.
(42) Cinar, M.; Yigit, A. A.; Yalcinkaya, I.; Oruc, E.; Duru, O.; Arslan, M. Cadmium induced changes on growth performance, some biochemical parameters and tissue in broilers: Effects of vitamin C and vitamin E. *Asian J. Anim. Vet. Adv.* **2011**, *6*, 923.
(43) Ambjørn, M.; Asmussen, J. W.; Lindstam, M.; Gotfryd, K.; Jacobsen, C.; Kiselyov, V. V.; Moestrup, S. K.; Penkowa, M.; Bock, E.; Berezin, V. Metallothionein and a peptide modeled after metallothionein, EmtinB, induce neuronal differentiation and survival through binding to receptors of the low-density lipoprotein receptor family. *J. Neurochem.* **2008**, *104* (1), 21−37.
(44) Eddins, D.; Petro, A.; Pollard, N.; Freedman, J. H.; Levin, E. D. Mercury-induced cognitive impairment in metallothionein-1/2 null mice. *Neurotoxicol. Teratol.* **2008**, *30* (2), 88−95.
(45) Dissanayake, I. H.; Bandaranayake, U.; Keerthirathna, L. R.; Manawadu, C.; Silva, R. M.; Mohamed, B.; Ali, R.; Peiris, D. C. Integration of in vitro and in-silico analysis of Caulerpa racemosa against antioxidant, antidiabetic, and anticancer activities. *Sci. Rep.* **2022**, *12* (1), 20848.
(46) Lescot, T.; Fulla-Oller, L.; Po, C.; Chen, X. R.; Puybasset, L.; Gillet, B.; Plotkine, M.; Meric, P.; Marchand-Leroux, C. Temporal and regional changes after focal traumatic brain injury. *J. Neurotrauma* **2010**, *27* (1), 85−94.
(47) McBride, D. W.; Szu, J. I.; Hale, C.; Hsu, M. S.; Rodgers, V. G.; Binder, D. K. Reduction of cerebral edema after traumatic brain injury using an osmotic transport device. *J. Neurotrauma* **2014**, *31* (23), 1948−1954.
(48) Zlokovic, B. V. The blood-brain barrier in health and chronic neurodegenerative disorders. *Neuron* **2008**, *57* (2), 178−201.
(49) Alipour, V.; Shabani, R.; Rahmani-Nia, F.; Vaseghi, S.; Nasehi, M.; Zarrindast, M. R. Effects of Treadmill Exercise on Social Behavior in Rats Exposed to Thimerosal with Respect to the Hippocampal Level of GluN1, GluN2A, and GluN2B. *J. Mol. Neurosci.* **2022**, *72* (6), 1345−1357.
(50) Noshadian, M.; Namvarpour, Z.; Amini, A.; Raoofi, A.; Atabati, H.; Sadeghi, Y.; Aliaghaei, A.; Abdollahifar, M. A. Alpha lipoic acid ameliorates THIM-induced prefrontal cell loss and abnormal enzymatically contents in the developing rat. *J. Chem. Neuroanat.* **2020**, *103*, 101727.
(51) Afsordeh, K.; Sadeghi, Y.; Amini, A.; Namvarpour, Z.; Abdollahifar, M. A.; Abbaszadeh, H. A.; Aliaghaei, A. Alterations of neuroimmune cell density and pro-inflammatory cytokines in response to thimerosal in prefrontal lobe of male rats. *Drug Chem. Toxicol.* **2019**, *42* (2), 176−186.

https://doi.org/10.1021/acsomega.3c07239
ACS Omega XXXX, XXX, XXX−XXX